Virology 517 (2018) 16–23

Contents lists available at ScienceDirect

Virology

journal homepage: www.elsevier.com/locate/virology

Aminopeptidase-N-independent entry of porcine epidemic diarrhea virus into Vero or porcine small intestine epithelial cells

Chun-Miao Ji, Bin Wang, Jiyong Zhou, Yao-Wei Huang*

Key Laboratory of Animal Virology of Ministry of Agriculture, College of Animal Sciences, Zhejiang University, Hangzhou 310058, Zhejiang, China

ARTICLE INFO

Keywords:
Porcine epidemic diarrhea virus (PEDV)
Aminopeptidase N (APN)
Receptor
CRISPR/Cas9
Vero cells
IPEC-J2 cells

ABSTRACT

A monkey cell line Vero (ATCC CCL-81) is commonly used for porcine epidemic diarrhea virus (PEDV) propagation *in vitro*. However, it is still controversial whether the porcine aminopeptidase N (pAPN) counterpart on Vero cells (Vero-APN) confers PEDV entry. We found that endogenous expression of Vero-APN was undetectable in the mRNA and the protein levels in Vero cells. We cloned the partial Vero-APN gene (3340-bp) containing exons 1 to 9 from cellular DNA and subsequently generated two APN-knockout Vero cell lines by CRISPR/Cas9 approach. PEDV infection of two APN-knockout Vero cells had the same efficiency as the Vero cells with or without neuraminidase treatment. A Vero cells stably expressing pAPN did not increase PEDV production. SiRNA-knockdown of pAPN in porcine jejunum epithelial cells had no effects on PEDV infection. The results suggest that there exists an additional cellular receptor on Vero or porcine jejunal cells independent of APN for PEDV entry.

1. Introduction

Porcine epidemic diarrhea virus (PEDV) is a positive-sense single stranded RNA virus belonging to the alphacoronavirus genus in the subfamily *Coronavirinae* of the family *Coronaviridae* (Pensaert and de Bouck, 1978; Song and Park, 2012). PEDV causes acute enteric disease in swine, characterized by acute vomiting and watery diarrhea, which has high mortality rates in newborn piglets (Huang et al., 2013; Pan et al., 2012). PEDV was discovered in the United Kingdom in early 1970s and was subsequently identified in many European and Asian countries (Lee et al., 2010; Li et al., 2012; Pensaert and Callebaut, 1974). PEDV field strains isolated before 2010 and the derived vaccine strains belong to genogroup 1 (G1) (Kocherhans et al., 2001). Since late 2010, variant PEDV strains (genogroup 2 [G2]) have emerged in China and Southeast Asia that were fatal to young pigs (Huang et al., 2013; Li et al., 2012). In May 2013, PEDV G2 strains suddenly emerged in the United States, wiping out more than 10% of America's pig population in one year (Huang et al., 2013; Tian et al., 2014). PEDV, together with the other newly emerged swine enteric coronaviruses such as porcine deltacoronavirus (PDCoV) and swine enteric alphacoronavirus (SeACoV), are considered serious threats to the pork industry in Asia currently (Jung et al., 2016; Pan et al., 2017).

Aminopeptidase N (APN or CD13) is a type II zinc metalloprotease that mediates various cellular processes, including antigen presentation, cell differentiation, cell motility and coronavirus entry (Luan and Xu, 2007). Porcine APN (pAPN) was first identified as a major receptor for a porcine enteropathogenic alphacoronavirus, transmissible gastroenteritis virus (TGEV) (Delmas et al., 1992). A related human alphacoronavirus, HCoV-229E, utilizes the human APN (hAPN) to enter host cells (Yeager et al., 1992). The interactions between TGEV/HCoV-229E and pAPN/hAPN are highly natural host specific, in which TGEV can use pAPN but not hAPN as its cellular receptor, and HCoV-229E can use hAPN but not pAPN (Kolb et al., 1996). It was reported that transfection and expression of pAPN was sufficient to confer PEDV infection to a non-permissive canine kidney MDCK cell line, indicating pAPN is likely a functional receptor for PEDV as well (Li et al., 2007). Moreover, transgenic mice expressing pAPN confer susceptibility to PEDV (Park et al., 2015). It was also reported that, unlike TGEV or HCoV-229E, PEDV spike protein-mediated pseudovirus was able to enter non-permissive canine kidney MDCK cells exogenously expressing either hAPN or pAPN, suggesting that the PEDV-APN interaction is not species specific (Liu et al., 2015). Correspondingly, PEDV can infect various cell lines from human, monkey, pig and bat species (Liu et al., 2015), but whether species-specific APN functions as the PEDV entry receptor on the respective cell line has not been investigated. However, most recently, two groups independently demonstrated that neither hAPN nor pAPN is the functional receptor for PEDV by using more comprehensive analyses, including knockout of endogenous expression of hAPN or pAPN in human or porcine cell lines by the Clustered Regularly Interspaced Short Palindromic Repeats (CRISPR)/CRISPR-

* Correspondence to: College of Animal Sciences, Zhejiang University, Zijingang Campus, 866 Yuhangtang Road, Hangzhou 310058, Zhejiang, China.
E-mail address: yhuang@zju.edu.cn (Y.-W. Huang).

https://doi.org/10.1016/j.virol.2018.02.019
Received 8 October 2017; Received in revised form 21 February 2018; Accepted 22 February 2018
Available online 02 March 2018
0042-6822/

associated protein-9 nuclease (Cas9) system (Li et al., 2017; Shirato et al., 2016).

An African green monkey (*Chlorocebus sabaeus*) kidney cell line, Vero (ATCC CCL-81), is commonly used for PEDV adaption and culture in the presence of trypsin *in vitro* for research or vaccine production (Hofmann and Wyler, 1988; Pan et al., 2012). Green monkey specific APN expressed on Vero cells (Vero-APN/vAPN) may serve as the entry receptor for PEDV (Li et al., 2007). However, a few studies remarked Vero cells without APN expression, but no experimental evidences were provided in these publications (Li et al., 2016; Nam and Lee, 2010). Therefore, the aim of this study was to clarify the argument, investigating whether Vero-APN is indeed responsible for PEDV entry into Vero cells. Furthermore, we sought to test whether knockdown of pAPN expression on porcine small intestinal epithelial cell line, IPEC-J2, is correlated with PEDV infection in comparison with TGEV.

2. Results and discussion

We first aimed to confirm if the putative green monkey APN (vAPN) gene exists in Vero cellular genome DNA. The 5'-part of the vAPN gene (3,340 bp), which was not available on the public genome database, was cloned by genomic PCR from extracted Vero genomic DNA with a pair of PCR primers shared significant sequence homology with human, chimpanzee, rhesus monkey and pig APNs. As illustrated in Fig. 1, the partial cloned vAPN gene contains nine exons or coding DNA sequence (CDS). The start codon ATG is located at CDS1 having 617 base pair (bp), whereas the sizes of the other eight CDS (CDS2–9) vary from 66 to 155 bp (Fig. 1). The partial cloned vAPN gene and its encoding cDNA (1,572 bp in size) share 97.9% and 98.9% sequence homology with the available rhesus monkey APN gene and cDNA, respectively. Attempts to amplification of the entire or the 5'-partial vAPN mRNA by RT-PCR were failed. Therefore, we performed a quantitative real-time PCR (qRT-PCR) analysis to detect if vAPN mRNA is expressed endogenously in Vero cells. As a control we examined hAPN mRNA expression in Huh-7 cells. When we confirmed endogenous hAPN mRNA expression, which was in line with the previously publications (Li et al., 2017; Liu et al., 2015), relative quantification of vAPN mRNA level to the green monkey β-actin control in Vero cells did not give a convincingly positive value in a cell-culture period of 3 days (data not shown). The result indicated that vAPN mRNA was expressed under the detection limit or was deficient in expression.

We further examined endogenous and exogenous expression of APN in the protein level using a broadly reactive anti-APN antibody by immunofluorescence assay (IFA) and western blot (WB) analysis. For comparison, two recombinant APN expression plasmids were constructed. Plasmid pCI-pAPN harbored the full-length porcine APN cDNA (2,892 bp) whereas plasmid pRK-vAPN contained the nine CDS of vAPN without introns followed by a stop codon (1,575 bp) that were fused sequentially by overlapping PCR. Vero or Huh-7 cells were transfected with either of the two plasmids. At 48 hour post-transfection, transfected or untransfected cells were subjected to IFA or WB. Specific anti-APN fluorescence signal was detected in transfected Vero or Huh-7 cells as well as untransfected Huh-7 cells (though the intensity was weak), but not observed in untransfected Vero cells (Fig. 2A). The WB analysis was consistent with the IFA result, showing individual bands of distinct sizes representing the full-length APN (APN-FL) or the partial APN (vAPN-CDS1–9) in pCI-pAPN- or pRK-vAPN-transfected Vero cells, whereas no bands were detected in untransfected Vero cells (Fig. 2B). In contrast, Huh-7 cells displayed a band corresponding to APN-FL regardless whether transfection with pCI-pAPN- or pRK-vAPN or not (Fig. 2B). Theses results indicated that Huh-7 cells express hAPN endogenously while Vero cells probably do not express vAPN inherently.

To further examine the effects of anti-APN antibody on PEDV entry into these two cell lines, we carried out quantitative PEDV infection analysis with a recombinant PEDV-GFP (see "Materials and methods"). Either Vero or Huh-7 cells were infected efficiently by PEDV-GFP, showing clear GFP fluorescence co-localized with cytopathic effects (CPE), which could be assessed by counting the numbers of GFP-positive cell clusters (Fig. 3A). Moreover, PEDV-GFP infection of two cell lines could be neutralized by anti-PEDV-S IgM or IgG in a dose-dependent manner (Fig. 3B), indicating that it is an appropriate *in vitro* model for quantification of PEDV infection. When anti-APN antibody at 2 μg/ml or 20 mg/ml was incubated with the cells prior to PEDV-GFP infection, it did not block PEDV-GFP entry or infection in Vero cells at 12 or 24 hour post-infection (hpi; Fig. 3C). For Huh-7 cells, it was observed that pretreatment with the antibody significantly decreased GFP-positive cell cluster numbers at 12 hpi; however, there was no differences in comparison with untreated cells at 24 hpi (Fig. 3C). Shirato and his colleagues reported that pAPN promotes PEDV infection through its protease activity rather than its proposed receptor function (Shirato et al., 2016). Since the protease active sites are highly conserved between hAPN and pAPN (Delmas et al., 1994), it is hypothesized that the anti-APN antibody blocked PEDV infection by targeting the enzymatically catalytic sites of hAPN on Huh-7 cells in the early stage (0–12 hpi). The inhibited effect was likely diminished when PEDV continued to propagate and spread thereafter. These results demonstrated that anti-APN antibody had no effects on PEDV entry into Vero cells, probably due to the absence of vAPN expression.

In order to completely rule out the potential vAPN production in Vero cells that may be under the detection limit, we set out to generate vAPN-knockout cells using CRISPR/Cas9 system. A single-plasmid CRISPR/Cas9 approach was developed, in which two guide RNA (gRNA) molecules and the Cas9 enzyme followed by a puromycin resistance gene are simultaneously expressed (Fig. 4A). We designed a knockout strategy using an engineered pX480-vAPNKO plasmid by targeting the vAPN CDS1 with two gRNA/Cas9 complexes to delete a 160-bp fragment between nucleotides 290–449 downstream of the translation initiation site (Fig. 1). At 3 days post-transfection with the pX480-vAPNKO plasmid plus puromycin selection, the genomic DNA was isolated and tested for vAPN gene integrity by PCR. It was shown that two different cell pools (using the same approach in two batches) possessed the intended vAPN deletion fragment, displaying weak bands smaller than the intact CDS1 (Fig. 4B). From these cell pools, we generated single cell clones, designated as $vAPN^{KO1}$ and $vAPN^{KO2}$, by limiting dilution with puromycin selection again. However, the intended vAPN deletion fragment was not visible in the clone $vAPN^{KO1}$ (Fig. 4C). Sequence analysis of the PCR products of the clone $vAPN^{KO1}$ revealed that there was only a 5-bp deletion (nt 290–294) downstream of the fist Cas9 cleavage site (Fig. 4D). The single cell clone $vAPN^{KO2}$ displayed the intended vAPN deletion fragment that was subsequently confirmed to have the expected 160-bp deletion by sequencing (Fig. 4C and D). Nevertheless, either of the deletions in $vAPN^{KO1}$ or $vAPN^{KO2}$ would result in a frameshift of vAPN allele.

We next confirmed that these knockout cells, Vero-$vAPN^{KO1}$ and Vero-$vAPN^{KO2}$, were deficient in vAPN expression by IFA (Fig. 5A). Upon PEDV-GFP infection, both Vero-$vAPN^{KO1}$ and Vero-$vAPN^{KO2}$ cells

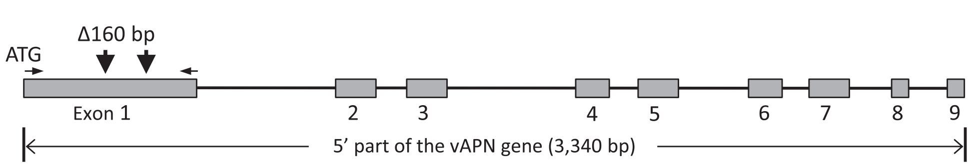

Fig. 1. Gene structure of the 5'-part of the vAPN gene containing the first nine exons (3,340 bp) determined in this study (GenBank accession number KX342855). Arrowheads indicate two Cas9 cleavage sites (nucleotides 290–449) downstream of the translation initiation site (ATG) within the exon 1 (CDS1). Deletion of a 160-bp fragment between these two sites will result in a frameshift. Arrows indicate PCR primers to assess gene integrity.

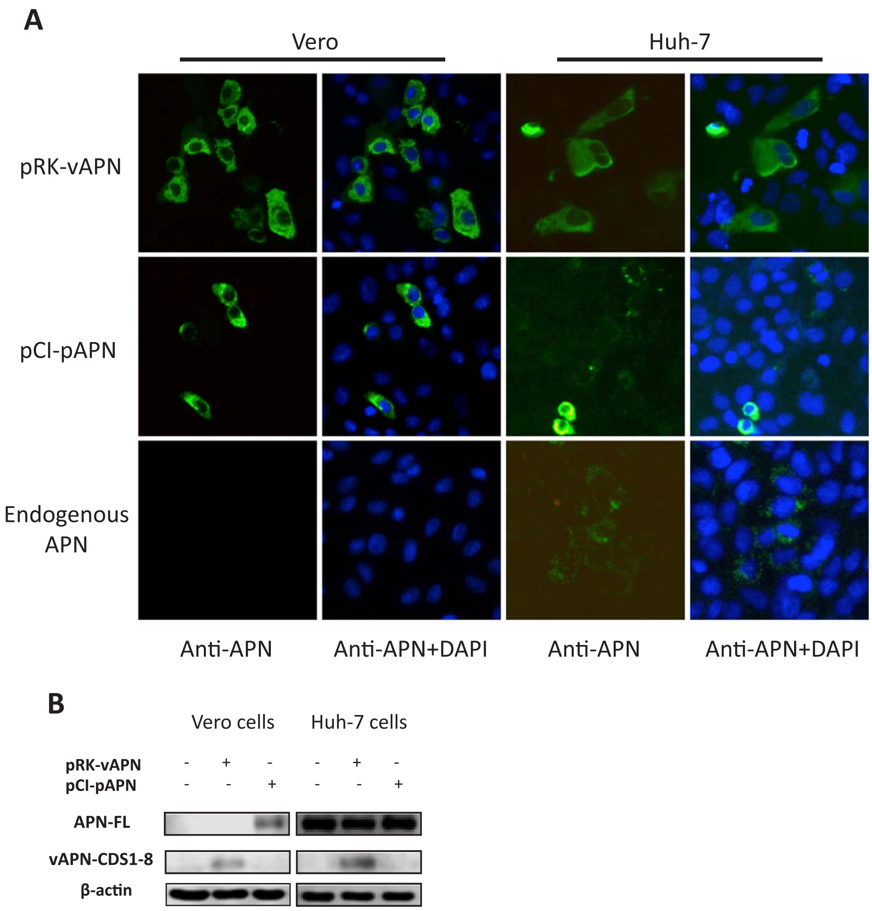

Fig. 2. Detection of endogenous expression or exogenous of APN in Vero or Huh-7 cells at 48 hours post-transfection. (A) Detection of endogenous expression or exogenous of APN in Vero cells or Huh-7 cells by IFA. For overexpression analysis, cells were transfected with the expression construct pRK-vAPN (containing the coding region from the first nine exons of vAPN) or pCI-pAPN (containing the complete porcine APN coding region). The polyclonal anti-APN antibody (abcam #93897) broadly cross-reacts with human, monkey or porcine APN. **(B)** Detection of the endogenous expression or exogenous of APN in Vero cells or in Huh-7 cells by western blotting. APN-FL: full-length pAPN (2,892 bp) expression; vAPN-CDS1–9: partial vAPN (1,575 bp) expression.

exhibited consequent CPE and GFP expression similar to normal Vero cells, indicating that vAPN knockout had no effects on PEDV entry and infection (Fig. 5B). Sialic acids such as Neu5Ac have been shown to be involved in PEDV entry as the co-receptor (Liu et al., 2015); therefore we examined whether there may be any interplay between sialic acids and APN for PEDV entry. Vero, Vero-vAPN^{KO1} and Vero-vAPN^{KO2} cells were infected with PEDV-GFP, respectively, in the presence of distinct concentrations of neuraminidase, which would cleave sialic acids on the cell surface. PEDV-GFP infection was inhibited slightly by neuraminidase treatment in a dose-dependent manner (Fig. 5C). However, there were no significant differences of overall effect of neuraminidase treatment on PEDV-GFP infection between normal Vero cells and knockout cells (Fig. 5C). These results indicated that vAPN knockout had no effects on potential association with sialic acids mediating PEDV entry.

It is reported that overexpression of pAPN in porcine kidney or testis cells slightly increased the production of PEDV, suggesting the role of pAPN in promoting PEDV replication (Nam and Lee, 2010; Shirato et al., 2016). We developed a stable Vero cell line expressing pAPN (Vero-pAPN; (Wang et al., 2018), and then determined whether Vero-pAPN cells could support PEDV-GFP propagation more efficiently in comparison with Vero cells. In agree with the previous findings, PEDV-GFP infectious titers increased during the early infection stage (0–24 hpi; Fig. 6). However, the peak virus titers were comparable between two cell lines (36–48 hpi; Fig. 6). The result indicated that although pAPN slightly facilitated PEDV replication in the early stage, it had limited effects on PEDV infection in Vero cells, probably due to the presence of an unidentified *bona fide* receptor.

PEDV infects pigs by targeting porcine small intestinal epithelial cells. Recently, a non-transformed, non-tumorigenic cell line named IPEC-J2, from jejunum epithelium isolated from a neonatal piglet, was characterized and used for studying porcine enteric virus-host interactions (Liu et al., 2010). Efficient PEDV-GFP or TGEV infection of IPEC-J2 cells was confirmed by optimizing the multiplicity of infection even treated with a small interfering RNA (siRNA) negative control (Fig. 7A and B), allowing us to use this cell line to study PEDV-pAPN interplay. However, our many attempts to knockout the pAPN in IPEC-J2 cells by CRISPR/Cas9 were failed, probably due to sensitivity of the cells to puromycin in the course of selection of single-cell clones (data not shown). We hence depleted pAPN expression by siRNA treatment (si-pAPN) in IPEC-J2 cells that were subsequently (24 hours post-siRNA transfection) infected with PEDV-GFP or TGEV. Immunoblot analysis of cell extracts harvested at 24 hpi verified that knockdown of the TGEV functional receptor, pAPN, reduced the abundance of the TGEV N protein relative to its level in cells treated with siNC (Fig. 7C). In accord with this, TGEV infection level decreased significantly as shown by IFA staining (Fig. 7A) and by measurement of the TGEV-positive cell clusters (Fig. 7B). In contrast, sipAPN knockdown did not affect PEDV-GFP infection as well as PEDV-N protein expression compared to the control (Fig. 7A-C), indicating that pAPN is the TGEV receptor but may not serve as the entry receptor for PEDV.

During the time of our study in progress, two independent studies described that neither hAPN nor pAPN is required for PEDV entry (Li et al., 2017; Shirato et al., 2016). In particular, Li et al. employed CRISPR/Cas9 technique to knockout either hAPN in Huh-7 cells or pAPN in ST cells, still resulting in efficient infection of PEDV in knockout cells, which convincingly demonstrated that PEDV infection does not utilize them as functional receptors (Li et al., 2017). Our study is in line with these results, providing additional evidences that the Vero cell line of green monkey origin does not express vAPN for PEDV entry and propagation, and that PEDV infection of the small intestinal epithelial cells is likely not associated with pAPN. The present study

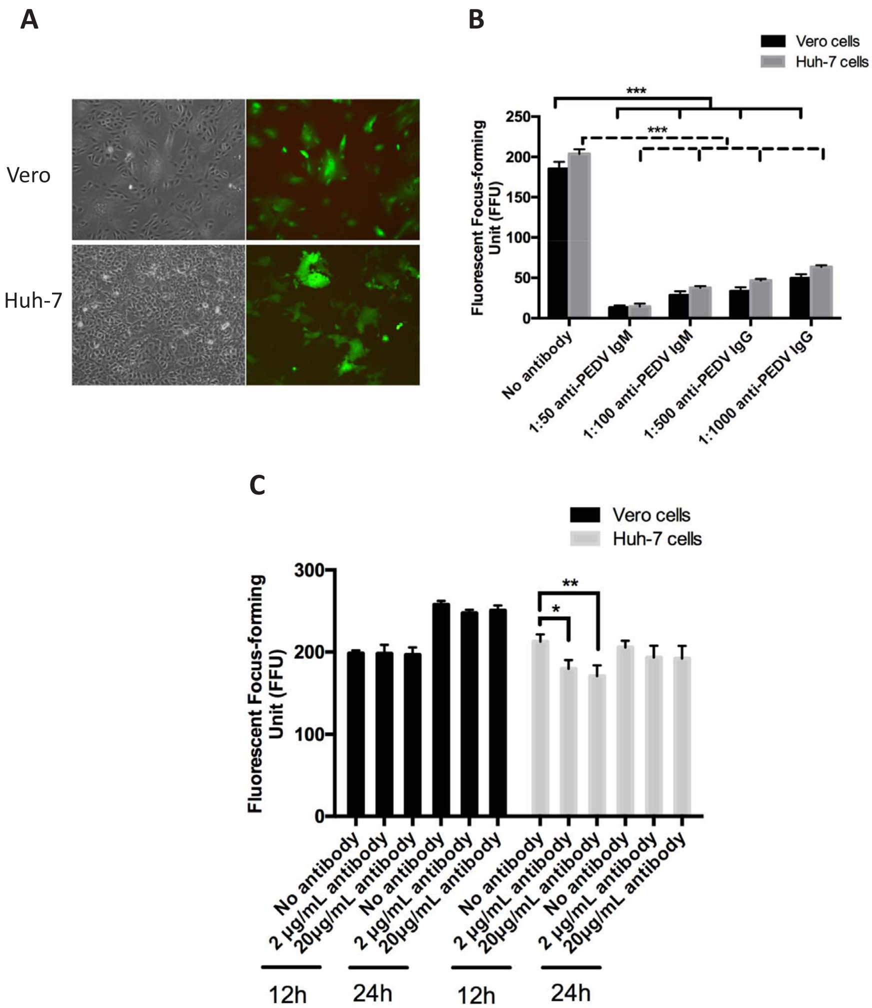

Fig. 3. PEDV-GFP infection of Vero or Huh-7 cells with or without treatment with anti-PEDV-S antibodies or anti-APN antibody. (A) Vero or Huh-7 cells were infected with PEDV-GFP at an MOI of 0.1 and observed under a fluorescence microscope at 24 hpi. **(B)** Vero or Huh7 cells were incubated with indicated mixture of PEDV-GFP (100 FFU) and dilutions of anti-PEDV-S IgM or IgG, and the numbers of GFP-positive cell clusters at 24 hpi were measured and compared, respectively. The figure represented mean values from three independent experiments, and error bars indicate standard deviation. **(C)** Cells were treated with 2 μg/ml or 20 μg/ml anti-APN antibody prior to PEDV-GFP infection, and the numbers of GFP-positive cell clusters at 12 or 24 hpi were measured, respectively.

should have broad biological significance, since the Vero cell is commonly used for PEDV propagation and vaccine production *in vitro*, and the porcine small intestine epithelial cells is the PEDV target *in vivo*. Furthermore, in our experiment using the PEDV non-susceptible BHK-21 or NIH-3T3 cells, we found that overexpression of pAPN did not confer PEDV-GFP entry or infection as well (data not shown). Therefore, these data collectively suggest that there exist additional cellular receptors independent of human, green monkey, and porcine APN for PEDV entry. Moreover, although PEDV is able to infect various cell lines of distinct species origin (Liu et al., 2015), even in duck species (Khatri, 2015), the other non-porcine and non-primate species-specific APNs (such as bat or duck APN) likely not functions as the PEDV entry receptor. Searching for the unknown PEDV functional receptor is still ongoing and should answer this enigma in the future.

3. Materials and methods

3.1. Cell lines and virus stocks

A monkey kidney cell line Vero (ATCC CCL-81), human hepatoma cell line Huh-7 and a swine testis cell line ST (ATCC CRL-1746) were grown in Dulbecco's modified Eagle medium (DMEM) supplemented with 10% fetal bovine serum (FBS) and 1% antibiotics at a 37°C incubator, respectively. A Vero cell line stably expressing the pAPN coding region (Vero-pAPN) was cultured in DMEM supplemented with 10 μg/ml puromycin and antibiotics (Wang et al., 2018). The IPEC-J2 cell line, from jejunum epithelium isolated from a neonatal piglet, was a generous gift from Dr. Lijuan Yuan at Virginia Tech, Blacksburg, VA (Liu et al., 2010). The IPEC-J2 cells were grown in DMEM supplemented with 5% FBS and 1% antibiotics.

A G2 PEDV Chinese strain, ZJU/G2/2013 (GenBank accession no. KU558701), was used in this study (Qin et al., 2017). The virus stocks of recombinant ZJU/G2/2013 expressing enhanced green fluorescent protein (GFP), designated PEDV-GFP, was generated by transfection of Vero cells with a DNA-launched PEDV infectious cDNA clone (Zhao et al., 2018), followed by two serial passages on Vero cells supplemented with 5 μg/ml trypsin (Sigma, Cat#T7186-50TAB, St Louis, MO, USA) and without FBS. The virus stocks were PEDV-GFP-containing supernatants without cell debris that were removed by centrifugation. The virus titers of PEDV-GFP were determined by endpoint dilutions as 50% tissue culture infective dose ($TCID_{50}$) on Vero cells. Virus stocks were stored at −80 °C until use. The PEDV-GFP infection efficiency in Vero, IPEC-J2, or Huh-7 cells was assessed by counting the numbers of GFP-positive cell clusters (quantified as fluorescent focus-forming unit [FFU]). TGEV Purdue strain was kindly provided by Dr. Rong Ye at Shanghai Medical College of Fudan University, which was propagated on ST cells (Pan et al., 2017). The TGEV infection efficiency in TGEV-infected-IPEC-J2 cells was also evaluated by counting the FFU numbers following immunofluorescence assay with a TGEV-specific antibody.

3.2. Genomic PCR and sequence analysis

A pairs of primers, vAPN-CDS1-F (5'- ATGGCCAAGGGCTTCTACAT TTCCAAG-3') and vAPN-CDS9-R (5'- CTCCTGCAGGTGGTCCCACAGG TTC-3'), were designed for amplification of the 5'-end region of the putative green monkey APN gene in Vero cells by one-step genomic

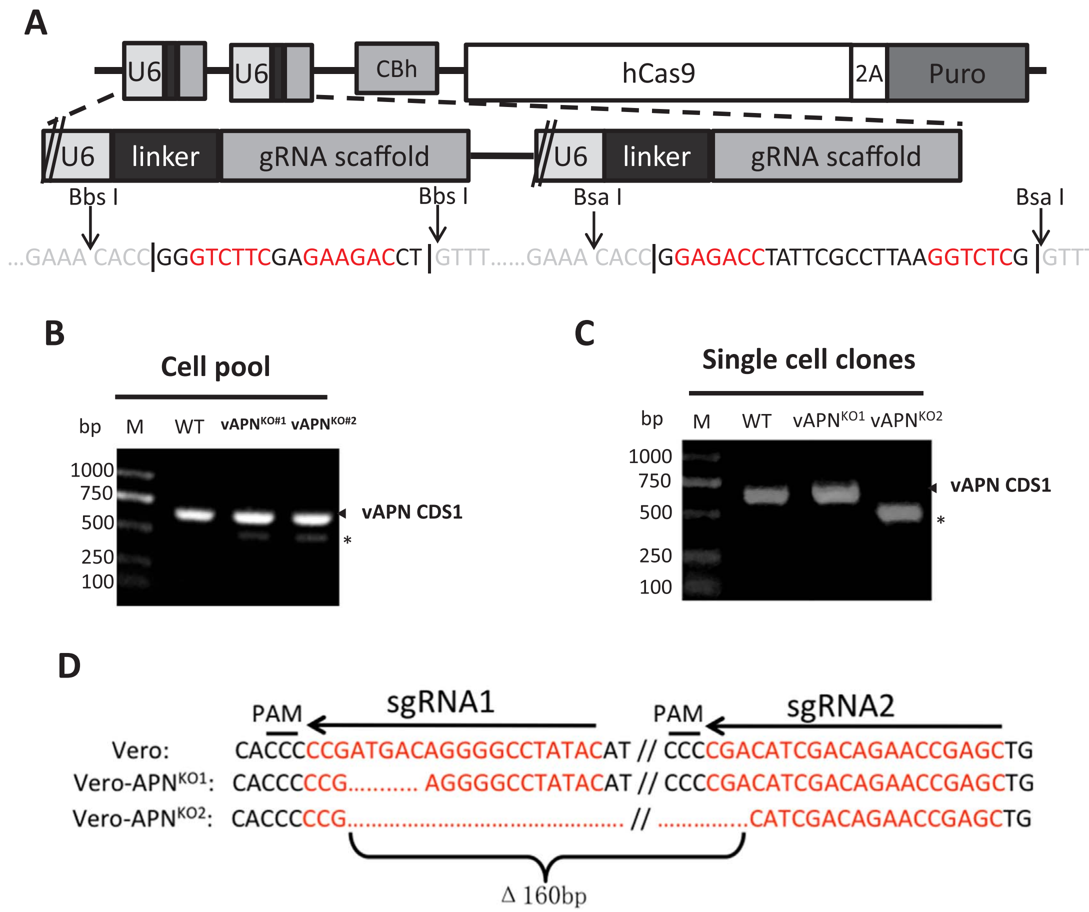

Fig. 4. Knockout of the putative vAPN gene expression by CRISPR/Cas9 in Vero cells. (A) Construction of a CRISPR/Cas9 backbone plasmid, pX480, containing two gRNA scaffolds used to generate vAPN knockout cells. Gene-specific gRNA sequences can be introduced by replacing the linker between the BbsI or BsaI recognition sequences. **(B)** Genomic DNA from mock-treated cells (WT), pX480-vAPNKO-transfected Vero cell pools (vAPN^{KO1} and vAPN^{KO2}) was used for PCR analysis of the vAPN gene integrity using primers flanking the Cas9 target sites in CDS1. Arrowhead indicates expected sizes of the PCR products of the intact CDS1, and the asterisk indicates the PCR product of a fragment possessing the intended deletion. **(C)** PCR analysis of vAPN gene integrity of single-cell clones, as described in panel B. **(D)** Sequence analysis of Vero, Vero-vAPN^{KO1}, and Vero-vAPN^{KO2} single-cell clones. The allele of the vAPN gene in Vero-vAPN^{KO1} possessed a 5-bp deletion. The allele of the vAPN gene in Vero-vAPN^{KO2} single-cell clone showed an expected 160-bp deletion. sgRNA: single-guide RNA.

PCR, based upon four published APN gene sequences from different species: *Homo sapiens* (human; Gene ID: 290), *Pan troglodytes* (chimpanzee; Gene ID: 467758), *Macaca mulatta* (rhesus monkey; Gene ID: 701117) and *Sus scrofa* (pig; Gene ID: 397520). The forward primer vAPN-CDS1-F contains the start codon ATG while the reverse primer vAPN-CDS9-R is complementary to the sequence at the 3'-end of the exon-9 of the rhesus monkey APN gene. Genomic PCR was performed with a KOD DNA polymerase (Toyobo, Japan) using 100 ng of extracted genomic DNA from Vero cells in a total volume of 50 µl. The PCR condition was 30 cycles of 98°C for 30 sec, 58°C for 30 sec, 68°C for 4 min with an initial denaturing of the template DNA at 94°C for 3 min and a final extension at 68°C for 7 min. The resulting fragment was cloned into a Zero pCR-Blunt vector (Thermo Fisher Scientific) by blunt-end cloning strategy followed by Sanger sequencing. Analysis and alignment of DNA and amino acid sequences were performed using Lasergene Package (DNASTAR Inc., Madison, WI).

3.3. Construction of the recombinant vectors expressing pAPN or Vero-APN and in vitro expression

The complete coding region of pAPN was amplified by one-step RT-PCR with primers PCI-APN-F (aggctagctACCATGGCCAAGGGATTCTACATTTCCAA) and PCI-APN-R (TTGTCGACTCAGCTGTGCTCTATGAACCAATTCAACA) using total RNAs extracted from porcine small intestine, and subsequently cloned into a pCI-neo vector (Promega) downstream of the CMV immediate-early enhancer/promoter using NheI and SalI restriction sites. The construct was sequenced to verify the identity and designated as pCI-pAPN. The nine exons, encoding the first 1572-bp of Vero-APN mRNA from the Vero-APN gene, were fused sequentially by overlapping PCR, and inserted into a pRK5 vector, to construct an expression vector, pRK-vAPN. Plasmids pCI-pAPN or pRK-vAPN were transiently transfected into Vero cells using Lipofectamine 3000 (Thermo Fisher Scientific) according to the manufacturer's protocol. Cells were cultured for 48 to 72 hours, and then applied to immunofluorescence assay or western blot to detect the expression of APN.

3.4. siRNA and siRNA transfections

The siRNA directed against pAPN (sipAPN: 5'-AACAAGCCCAGCUGGUAAA-3') or the negative control (siNC: 5'-UUCUCCGAACGUGUCACGU-3') was purchased from RiboBio (Guangzhou, China). The siRNA transfections in IPEC-J2 cells were performed using the Lipofectamine RNAiMAX transfection reagent (Thermo Fisher Scientific, USA) according to manufacturer's instructions. At 24 hour post-transfection, IPEC-J2 cells were infected with PEDV-GFP at an MOI (multiplicity of infection) of 5 or with TGEV (MOI = 1).

3.5. Immunofluorescence assay, western blot and quantitative real-time PCR

Transfected cells or APN-knockout Vero cells were washed 2 times with PBS, fixed with 4% paraformaldehyde in PBS for 20 min and then

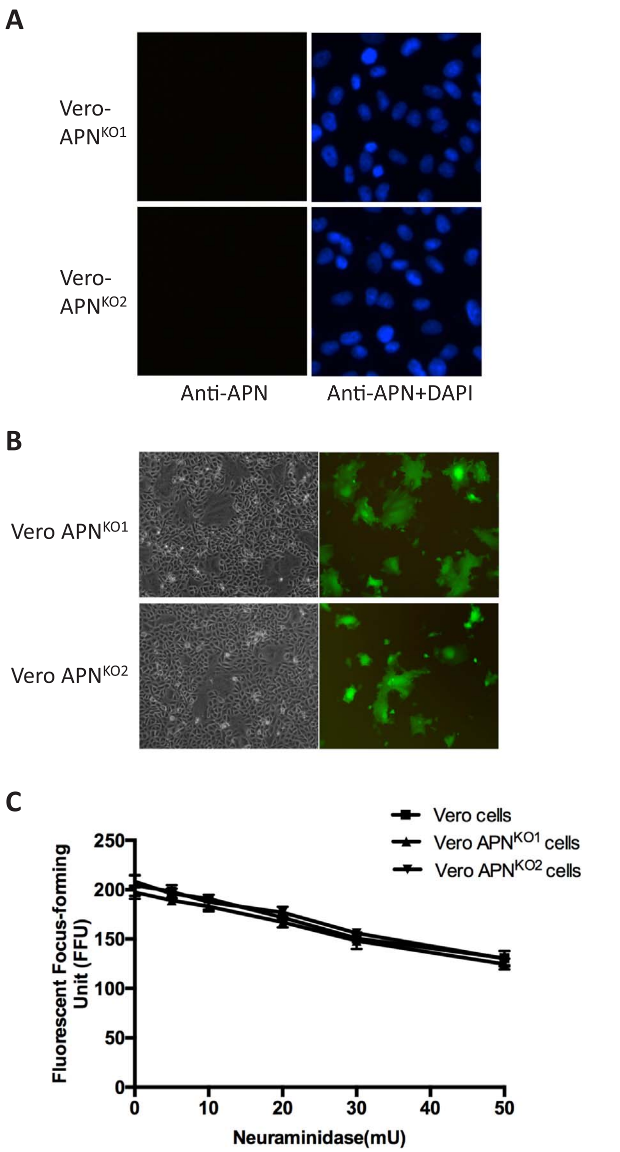

Fig. 5. No effects of vAPN knockout on PEDV-GFP infection in Vero cells. (A) No APN expression on either Vero-vAPN^{KO1} or Vero-vAPN^{KO2} cells, as confirmed by IFA. **(B)** Efficient PEDV infection of Vero-vAPN^{KO1} or Vero-vAPN^{KO2} cells. Cells were infected with PEDV-GFP at an MOI of 0.1 and observed under a fluorescence microscope at 24 hpi. **(C)** No effects of neuraminidase pre-treatment on vAPN knockout cells infected with PEDV-GFP. The numbers of GFP-positive cell clusters at 24 hpi were measured and compared.

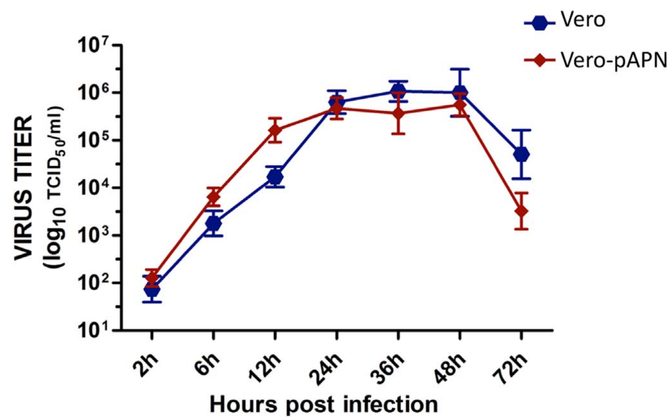

Fig. 6. Comparison of growth kinetics of PEDV-GFP between Vero and Vero-pAPN cells. Vero or Vero-pAPN cells were infected in triplicate with PEDV-GFP at an MOI =0.1. Cells were harvested at 2, 6, 12, 24, 36, 48, and 72 hpi, and virus titers ($TCID_{50}$/ml) were determined in triplicate on Vero cells. Error bars indicate standard deviation.

permeabilized with 0.5% Triton X-100 for 10 min. One hundred microliters of the polyclonal anti-APN antibody (abcam #93897), at a 1:100 dilution in PBS, was added over the cells and incubated for 1 hour at 37°C. Cells were washed trice with PBS and 100 µl FITC-labeled goat anti-rabbit IgG (Thermo Fisher Scientific) at a 1:100 dilution was then added. After 30 min incubation at 37°C, the cells were washed trice with PBS followed by 4',6-diamidino-2-phenylindole (DAPI) staining, and were visualized under a fluorescence microscope. For detection of TGEV infection in ST cells, at 24 hpi, TGEV-infected ST cells were stained with a rabbit anti-TGEV-nucleocapsid protein (N) polyclonal antibody (made in-house) as the primary antibody, and an Alexa Fluor 488-conjugated goat anti-rabbit IgG (Thermo Fisher Scientific, USA) as the secondary antibody followed by DAPI staining.

For western blot analysis of APN expression, pCI-pAPN or pRK-vAPN transfected cells, PEDV- or TGEV-infected IPEC-J2 cells were lysed in 125 µl CelLytic M lysis buffer (Sigma) per 10^6 cells, respectively. Protein extracts were collected, aliquated and frozen at −20°C. Samples were resolved on SDS-PAGE and transferred onto polyvinylidene difluoride (PVDF) membrane that was subsequently blocked with Tris-buffered saline (TBS) containing 3% bovine serum albumin (BSA) overnight at 4°C. Proteins were detected using the anti-APN antibody at a 1:200 dilution followed by incubation with horseradish peroxidase (HRP)-conjugated anti-rabbit IgG (Thermo Fisher Scientific). Detection of the N protein expression of PEDV or TGEV in infected IPEC-J2 cells were conducted by using the anti-PEDV-N monoclonal antibody (purchased from Medgene Labs, Brookings, SD, USA) or the anti-TGEV-N polyclonal antibody.

For qRT-PCR analysis, total RNA was extracted from cell lysis using an AxyPrep Multisource Total RNA Miniprep Kit (Axygen). Detection of mRNA expression levels of hAPN in Huh-7 cells or vAPN in Vero cells by qRT-PCR was performed using TransScript Green One-Step qRT-PCR SuperMix (Transbionovo, Beijing, China) with primers hAPN-qPCR-F (5'-GGACAGCCAGTATGAGAT-3') and hAPN-qPCR-R (5'-GGATAAGCG TGATGTTGAA-3'), or primers vAPN-qPCR-F (5'-TGAGATGGACAGTGA GTTC-3') and vAPN-qPCR-R (5'-GTGGATAAGCGTGATGTTG-3'). Relative quantification was expressed as $2^{-\Delta Ct}$, where Ct is the difference between the main Ct value of the sample in triplicate and that of an endogenous human β-actin (primers 5'-ATGACCAACAAGTGTCTCC TCC-3' and 5'-GGAATCCAAGCAAGTTGTAGCTC-3') or green monkey β-actin control (primers 5'-CCTGGCACCCAGCACAAT-3' and 5'-GGGCCG GACTCGTCATAC-3').

3.6. Treatment with anti-PEDV spike (S) protein antibodies, anti-APN antibody or neuraminidase

Cells were incubated with the anti-APN antibody at 2 µg/ml or 20 mg/ml or neuraminidase (Sigma) at concentrations of 5, 10, 20, 30 or 50 mU in DMEM for 1 h at 37°C prior to PEDV-GFP infection. For neutralizing test, serial dilutions (1:50, 1:100, 1:500 or 1:1000) of anti-PEDV-S IgM (Medgene Labs, Brookings, SD, USA) or anti-PEDV-S IgG (JBT, Korea) were each mixed with 100 FFU of PEDV-GFP, incubated at 37 °C for 1 h to form virus-antibody complexes, and added to Vero cells. Cells were fixed in 4% paraformaldehyde at appropriate time points, and GFP-positive cells were counted.

3.7. Generation of APN knockout (KO) cell lines by using CRISPR/Cas9 system

We first constructed a Cas9 backbone cloning vector, named pX480, harboring two guide RNA (gRNA) expression cassettes as well as a 2A-puromycin resistance gene inserted following the human Cas9 gene based upon the pX330 vector (Addgene) (Ran et al., 2013). The used primers and construction details will be available upon request. The pX480 vector was digested with BbsI and BsaI sequentially and ligated

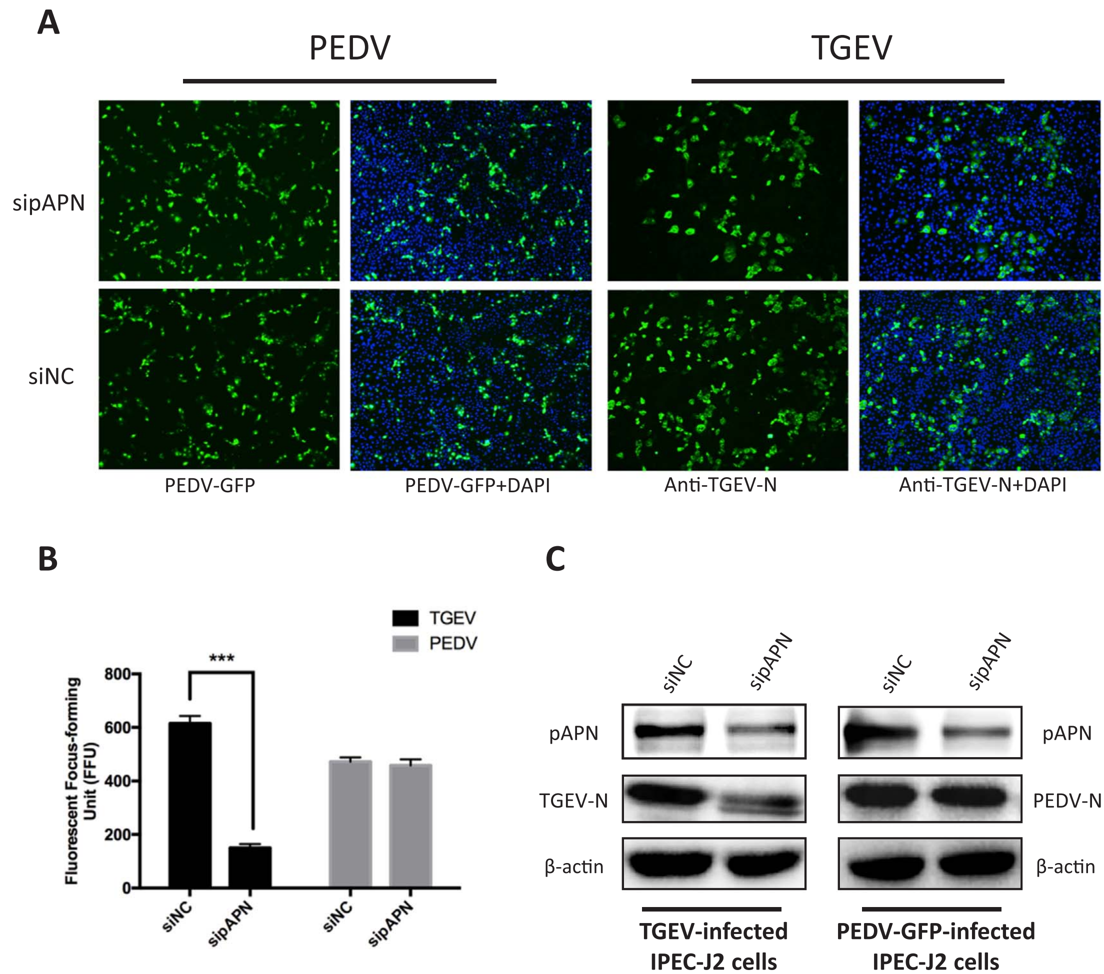

Fig. 7. Effects of pAPN knockdown on PEDV-GFP or TGEV infection in IPEC-J2 cells. (A) IPEC-J2 cells were transfected with sipAPN or siNC for 24 hours followed by infection with either PEDV-GFP (MOI = 5) or TGEV (MOI = 1). Observation of GFP expression in PEDV-GFP-infected cells or detection of TGEV-N protein expression in TGEV-infected cells by IFA was performed at 24 hpi. **(B)** The numbers of PEDV- and TGEV-positive cell clusters were measured from (A), respectively. The result represented mean values from three independent experiments, and error bars indicate standard deviation (***: $p < 0.001$). (C) Detection of expression of pAPN, TGEV-N or PEDV-N in siRNA-treated cells followed by virus infection (24 hpi) by western blotting.

with annealed protospacer oligoDNAs (nucleotides 284–306, 5'-CCGATGACAGGGGCCTATAC-3' and nucleotides 444–466, 5'-CGACATCGACAGAACCGAGC-3') specific for the vAPN CDS1 sequences to obtain a single-plasmid pX480-vAPNKO. Vero-APN knockout cells were generated by CRISPR/Cas9 gene editing as described (Ran et al., 2013). Single cell clones of vAPN knockout cells were obtained by limiting dilution and genotyped by PCR and DNA sequencing.

3.8. Nucleotide sequence accession numbers

The sequences of the pAPN cDNA and the partial Vero-APN gene determined in this study have been deposited in GenBank under accession nos. KX342854 and KX342855, respectively.

Acknowledgments

This work was supported by the National Key Research and Development Program of China (2016YFD0500102), the National Natural Science Foundation of China (31572518), the Key Research and Development Program of Zhejiang province (2015C02021), and the Zhejiang Provincial Science Foundation for Distinguished Young Scholars (LR14C180001).

References

Delmas, B., Gelfi, J., Kut, E., Sjostrom, H., Noren, O., Laude, H., 1994. Determinants essential for the transmissible gastroenteritis virus-receptor interaction reside within a domain of aminopeptidase-N that is distinct from the enzymatic site. Journal of virology 68, 5216–5224.

Delmas, B., Gelfi, J., L'Haridon, R., Vogel, L.K., Sjostrom, H., Noren, O., Laude, H., 1992. Aminopeptidase N is a major receptor for the entero-pathogenic coronavirus TGEV. Nature 357, 417–420.

Hofmann, M., Wyler, R., 1988. Propagation of the virus of porcine epidemic diarrhea in cell culture. Journal of clinical microbiology 26, 2235–2239.

Huang, Y.W., Dickerman, A.W., Pineyro, P., Li, L., Fang, L., Kiehne, R., Opriessnig, T., Meng, X.J., 2013. Origin, evolution, and genotyping of emergent porcine epidemic diarrhea virus strains in the United States. mBio 4, e00737–00713.

Jung, K., Hu, H., Saif, L.J., 2016. Porcine deltacoronavirus infection: Etiology, cell culture for virus isolation and propagation, molecular epidemiology and pathogenesis. Virus research 226, 50–59.

Khatri, M., 2015. Porcine epidemic diarrhea virus replication in duck intestinal cell line. Emerging infectious diseases 21, 549–550.

Kocherhans, R., Bridgen, A., Ackermann, M., Tobler, K., 2001. Completion of the porcine epidemic diarrhoea coronavirus (PEDV) genome sequence. Virus genes 23, 137–144.

Kolb, A.F., Maile, J., Heister, A., Siddell, S.G., 1996. Characterization of functional domains in the human coronavirus HCV 229E receptor. The Journal of general virology 77 (Pt 10), 2515–2521.

Lee, D.K., Park, C.K., Kim, S.H., Lee, C., 2010. Heterogeneity in spike protein genes of porcine epidemic diarrhea viruses isolated in Korea. Virus research 149, 175–182.

Li, B.X., Ge, J.W., Li, Y.J., 2007. Porcine aminopeptidase N is a functional receptor for the PEDV coronavirus. Virology 365, 166–172.

Li, W., Li, H., Liu, Y., Pan, Y., Deng, F., Song, Y., Tang, X., He, Q., 2012. New variants of porcine epidemic diarrhea virus, China, 2011. Emerging infectious diseases 18, 1350–1353.

Li, W., Luo, R., He, Q., van Kuppeveld, F.J.M., Rottier, P.J.M., Bosch, B.J., 2017.

Aminopeptidase N is not required for porcine epidemic diarrhea virus cell entry. Virus research 235, 6–13.
Li, W., van Kuppeveld, F.J., He, Q., Rottier, P.J., Bosch, B.J., 2016. Cellular entry of the porcine epidemic diarrhea virus. Virus research 226, 117–127.
Liu, C., Tang, J., Ma, Y., Liang, X., Yang, Y., Peng, G., Qi, Q., Jiang, S., Li, J., Du, L., Li, F., 2015. Receptor usage and cell entry of porcine epidemic diarrhea coronavirus. Journal of virology 89, 6121–6125.
Liu, F., Li, G., Wen, K., Bui, T., Cao, D., Zhang, Y., Yuan, L., 2010. Porcine small intestinal epithelial cell line (IPEC-J2) of rotavirus infection as a new model for the study of innate immune responses to rotaviruses and probiotics. Viral immunology 23, 135–149.
Luan, Y., Xu, W., 2007. The structure and main functions of aminopeptidase N. Current medicinal chemistry 14, 639–647.
Nam, E., Lee, C., 2010. Contribution of the porcine aminopeptidase N (CD13) receptor density to porcine epidemic diarrhea virus infection. Veterinary microbiology 144, 41–50.
Pan, Y., Tian, X., Li, W., Zhou, Q., Wang, D., Bi, Y., Chen, F., Song, Y., 2012. Isolation and characterization of a variant porcine epidemic diarrhea virus in China. Virology journal 9, 195.
Pan, Y., Tian, X., Qin, P., Wang, B., Zhao, P., Yang, Y.L., Wang, L., Wang, D., Song, Y., Zhang, X., Huang, Y.W., 2017. Discovery of a novel swine enteric alphacoronavirus (SeACoV) in southern China. Veterinary microbiology 211, 15–21.
Park, J.E., Park, E.S., Yu, J.E., Rho, J., Paudel, S., Hyun, B.H., Yang, D.K., Shin, H.J., 2015. Development of transgenic mouse model expressing porcine aminopeptidase N and its susceptibility to porcine epidemic diarrhea virus. Virus research 197, 108–115.
Pensaert, M.B., Callebaut, P.E., 1974. Characteristics of a coronavirus causing vomition and wasting in pigs. Archiv fur die gesamte Virusforschung 44, 35–50.
Pensaert, M.B., de Bouck, P., 1978. A new coronavirus-like particle associated with diarrhea in swine. Archives of virology 58, 243–247.
Qin, P., Li, H., Wang, J.W., Wang, B., Xie, R.H., Xu, H., Zhao, L.Y., Li, L., Pan, Y., Song, Y., Huang, Y.W., 2017. Genetic and pathogenic characterization of a novel reassortant mammalian orthoreovirus 3 (MRV3) from a diarrheic piglet and seroepidemiological survey of MRV3 in diarrheic pigs from east China. Veterinary microbiology 208, 126–136.
Ran, F.A., Hsu, P.D., Wright, J., Agarwala, V., Scott, D.A., Zhang, F., 2013. Genome engineering using the CRISPR-Cas9 system. Nat Protoc 8, 2281–2308.
Shirato, K., Maejima, M., Islam, M.T., Miyazaki, A., Kawase, M., Matsuyama, S., Taguchi, F., 2016. Porcine aminopeptidase N is not a cellular receptor of porcine epidemic diarrhea virus, but promotes its infectivity via aminopeptidase activity. The Journal of general virology 97, 2528–2539.
Song, D., Park, B., 2012. Porcine epidemic diarrhoea virus: a comprehensive review of molecular epidemiology, diagnosis, and vaccines. Virus genes 44, 167–175.
Tian, P.F., Jin, Y.L., Xing, G., Qv, L.L., Huang, Y.W., Zhou, J.Y., 2014. Evidence of recombinant strains of porcine epidemic diarrhea virus, United States, 2013. Emerging infectious diseases 20, 1735–1738.
Wang, B., Liu, Y., Ji, C.M., Yang, Y.L., Liang, Q.Z., Zhao, P., Xu, L.D., Lei, X.M., Luo, W., Qin, P., Zhou, J., Huang, Y.W., 2018. Porcine deltacoronavirus engages alphacoronavirus TGEV functional receptor porcine aminopeptidase N for infectious cellular entry Manuscript in preparation.
Yeager, C.L., Ashmun, R.A., Williams, R.K., Cardellichio, C.B., Shapiro, L.H., Look, A.T., Holmes, K.V., 1992. Human aminopeptidase N is a receptor for human coronavirus 229E. Nature 357, 420–422.
Zhao, P., Wang, B., Ji, C.M., Cong, X., Wang, M., Huang, Y.W., 2018. Identification of a peptide derived from the heptad repeat 2 region of the porcine epidemic diarrhea virus (PEDV) spike glycoprotein that is capable of suppressing PEDV entry and inducing neutralizing antibodies. Antiviral research 150, 1–8.